Proceedings of the 9th U.S. National and 10th Canadian Conference on Earthquake Engineering
Compte Rendu de la 9ième Conférence Nationale Américaine et
10ième Conférence Canadienne de Génie Parasismique
July 25-29, 2010, Toronto, Ontario, Canada • Paper No 1502

INVESTIGATION OF BASIN AND DIRECTIVITY EFFECTS IN BROADBAND SIMULATED GROUND MOTIONS

L. M. Star[1], J. P. Stewart[1], and R. W. Graves[2]

Abstract

The ShakeOut exercise utilized broadband simulated ground motions for an M_w 7.8 scenario rupture on the San Andreas fault. We compare motions for the ShakeOut event, two ShakeOut permutations with different hypocenter locations, and a M_w 7.15 Puente Hills blind thrust event beneath downtown Los Angeles, to median predictions from the empirical NGA ground motion prediction equations. In work reported elsewhere the simulated motions were found to attenuate faster with distance than is predicted by the NGA models for most periods. After removing the distance attenuation bias, we find the simulated motions have a depth-dependent basin response similar to the NGA models, but also show complex effects in which stronger basin response occurs when the fault rupture transmits energy into a basin at low angle. Rupture directivity effects scale with the isochrone parameter.

Introduction

Earthquake ground motions are generally evaluated for engineering applications using empirical ground motion prediction equations (GMPEs), which capture the average effects of earthquake source, travel path, and site effects. The Next-Generation Attenuation (NGA) GMPEs (Power et al., 2008) represent the standard of practice for ground motion prediction from shallow crustal earthquakes in active regions.

Simulated ground motions have the potential to provide a valuable supplement to empirical methods, especially for large magnitudes and close site-source distances (e.g., $M_w > 7.5$ and distance < 20 km) for which recordings are sparse, especially for strike-slip earthquakes. Simulations may also be useful for ground motion evaluation under certain unique site-specific conditions for which records may be unavailable. One such situation is downtown Los Angeles, where blind thrust faults underlie a deep sedimentary basin. Complex 3D effects might be anticipated for such conditions that cannot be assessed from GMPEs.

Simulation procedures that capture complex source features (such as spatially variable slip distributions, rise times, and rupture velocities), path effects (geometric spreading and crustal damping), and site effects (wave propagation through basins and shallow site response) can help fill this need. However, such techniques have not found significant practical applications to date in the western United States because of a general sense among engineers that the simulated motions have not been adequately validated.

Star et al. (2010) presented a procedure that checks key attributes of simulated motions relative to empirical observation, as represented by appropriate GMPEs. That procedure was applied to four simulated events that are described in the following section. The simulated motions were found to attenuate faster with distance than the GMPEs. A coefficient in the

[1] University of California Los Angeles, Civil and Environ. Engrg. Dept., 5731 Boelter Hall, Los Angeles, CA 90095-1593. Email: lcoyne@ucla.edu; jstewart@seas.ucla.edu,
[2] URS Corporation, 566 El Dorado St., Pasadena CA 91101-2560, Email: Robert_Graves@URScorp.com

GMPE distance attenuation term was adjusted to remove the bias. This paper presents a follow up on that work, utilizing residuals of the modified GMPEs to investigate basin and directivity effects implied by the simulated data.

Attributes of the Simulated Events

The ShakeOut Scenario earthquake is an M_w 7.8 event on the southernmost 300 km of the San Andreas Fault (Porter et al. 2010). As shown in Figure 1, the ShakeOut event ruptures from south to north. We also examine two alternative realizations of the rupture scenario with hypocenters located at the center (bilateral rupture) and north end of the fault (rupture towards south).

Figure 1. Map of Southern California showing the ruptured southern section of the San Andreas fault (red) in the ShakeOut event along with the three considered hypocenter locations as well as the Puente Hills fault (blue).

The Puente Hills scenario is an M_w 7.15 event on a thrust fault beneath downtown Los Angeles (Graves and Somerville, 2006), which is shown in Figure 1. The fault dips at 27 degrees downward towards the north. The full length and width of the fault is assumed to rupture updip from near the base of the fault plane to within 3 km of the ground surface.

The simulations use a hybrid procedure in which short period ground motions are computed semi-stochastically and long period motions are computed from a physics-based deterministic procedure (Graves and Pitarka, 2004). The deterministic procedure considers both heterogeneous fault rupture and wave propagation through the crust and the sedimentary basins in and around Los Angeles. Basins are represented using SCEC Community Velocity Model version 4 (CVM4). The CVM4 is a 3D seismic velocity structure model which can be queried to give V_p, V_s, and density for a given latitude, longitude and depth (www.data.scec.org/3Dvelocity, Magistrale et al., 2000). The effects of relatively shallow site condition, as represented by shear wave velocity in the upper 30 m (V_{s30}), are accounted for using the empirical site amplification model of Campbell and Bozorgnia (2008) combined with V_{s30} maps by Wills et al. (2000). More information about the rupture model and simulation methodology is available in Graves et al. (2008).

Verification of Simulated Motions

Residuals between the intensity measures from the simulation procedure and a particular GMPE as calculated as follows:

$$R_i(T) = \ln\left(S_a(T)\right)_{sim,i} - \ln\left(S_a(T)\right)_{GMPE,i} \quad (1)$$

where index i refers to a particular location where ground motions were simulated (latitude and longitude), $S_a(T)_{sim,i}$ refers to the 5% damped spectral acceleration of the simulated motion for oscillator period T at location i, $S_a(T)_{GMPE,i}$ refers to the median spectral acceleration for location i predicted by a GMPE considering the earthquake magnitude, site-source distance, and site condition, and R_i is the residual in natural logarithmic units. In this paper, we utilize modified GMPEs that capture the faster distance attenuation of the simulated data relative to the original GMPE. The original GMPEs are those of Abrahamson and Silva (2008), Boore and Atkinson (2008), Campbell and Bozorgnia (2008), and Chiou and Youngs (2008) GMPEs. We use shorthand AS, BA, CB, and CY subsequently to refer to those GMPEs.

Basin and Directivity Effects

Parameterization of Basin Effects

The primary parameter used to characterize basin effects is Z_x, the depth to an isosurface having shear wave velocity of x. The NGA relations use two depth parameters: $Z_{1.0}$ = depth to V_s = 1.0 km/s (AS and CY) and $Z_{2.5}$ = depth to V_s = 2.5 km/s (CB). The BA model does not include a separate basin term. For the calculation of residuals, basin depths were queried at the locations of simulated motions using the SCEC Community Velocity Model version 4 (CVM4).

Choi et al. (2005) suggest a second binary parameter describing basin location relative to the source fault. They designated basins at least partially overlying or adjacent to the source as having coincident source and basin locations (CBL basins) and basins away from the source as having distinct source and basin locations (DBL basins). CBL basins had depth-dependent long-period ground motions, whereas DBL basins had depth-independent ground motions. This was found from both simulated and actual ground motions from modest-sized earthquakes in and around the Los Angeles basin and San Fernando Valley. To examine differences in ground motions for CBL and DBL basins using the ShakeOut and Puente Hills simulations, it is necessary to identify sites within the various basins of southern California, which in turn requires definition of basin boundaries. A contour at $Z_{2.5}$ = 1.0 km generally provides a convenient definition of the basin boundary. However, because the San Bernardino basin is relatively shallow, we chose to define this particular basin boundary using a contour at $Z_{1.0}$ = 0.3 km. Figure 2 shows the southern California basins and their boundaries using the CVM4 model. For the ShakeOut scenarios, DBL basins include Los Angeles, San Fernando, Ventura, Off Shore, and Kern County, whereas CBL basins are Imperial and San Bernardino. For the Puente Hills scenario, the Los Angeles basin is a CBL basin, and DBL basins are San Bernardino, San Fernando and Ventura.

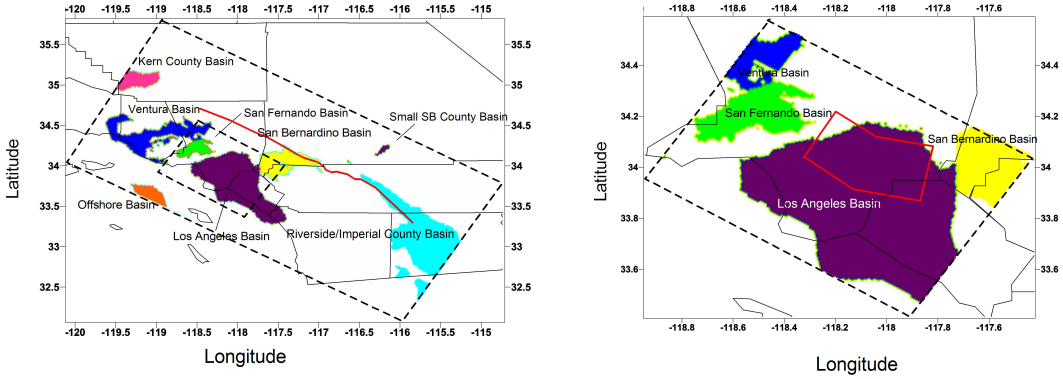

Figure 2. Southern California basins relative to fault traces producing ShakeOut and Puente Hills rupture scenarios

Parameterization of Directivity Effects

The propagation of fault rupture towards a site at a rupture velocity near the crustal shear wave speed causes seismic energy from the rupture to arrive in a large pulse. Sites located down-strike (for a strike slip fault) or up-dip (for a dip slip fault) from the hypocenter experience this effect, which is known as forward directivity. Sites in the forward directivity region on average exhibit stronger ground motions, as measured by the average of the horizontal components, than predicted by GMPEs. The effect is most noticeable at long periods, and tends to be concentrated at a pulse period that is loosely correlated to the earthquake magnitude (Baker 2007). Forward directivity motions can be polarized in the fault normal (FN) direction, meaning that the FN component is stronger than the average horizontal. Watson-Lamprey and Boore (2007) show that the FN azimuth generally aligns with the maximum component of motion for sites within approximately 3 km of the fault, whereas at larger distances the azimuth of the maximum component is arbitrary.

Spudich and Chiou (2008) (denoted SC) relate rupture directivity effects, as observed in the average horizontal component of ground motions, to the Isochrone Directivity Predictor (*IDP*):

$$IDP = C \cdot S \cdot R_{ri} \qquad (2)$$

In Eq. (2), C is the normalized form of the isochrone velocity ratio. It captures the amplification due to rupture propagation around a fault. The role of C is similar to that of the well-known $\cos(\theta)$ term from the model of Somerville et al. (1997) (for a strike-slip fault, θ is the angle between the fault strike and a line drawn from the epicenter to the site). Parameter S describes the amount of the fault that is rupturing toward the site, similar to parameter X from Somerville et al. (1997) (for a strike-slip fault, X is the fraction of the fault rupturing towards the site). Parameter R_{ri} is the scalar radiation pattern, which is approximated by that for a single point source. Figure 3 shows maps of IDP for the ShakeOut south hypocenter and Puente Hills events.

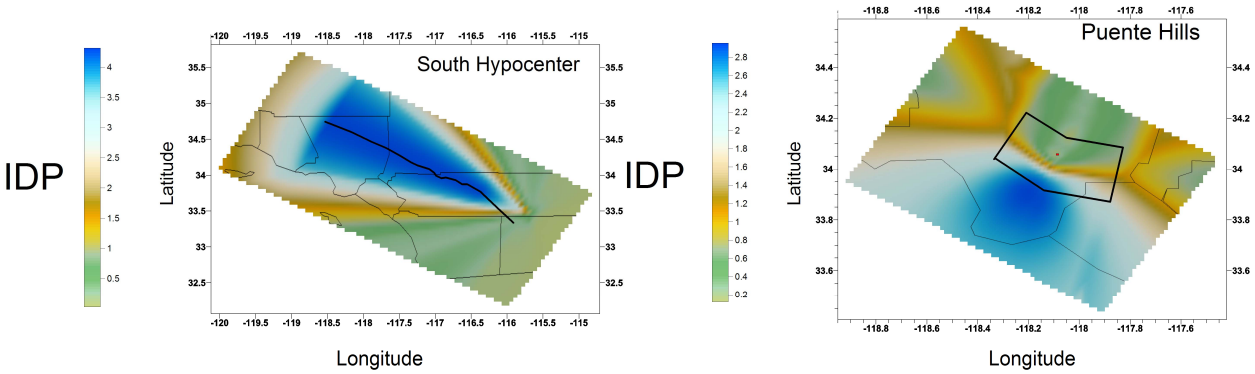

Figure 3. Maps of southern California showing IDP for ShakeOut south hypocenter and Puente Hills scenarios.

None of the NGA GMPEs include a directivity term. However, SC developed empirical models for a directivity correction in the form of:

$$f_D = f_R \cdot f_M \left(a + b \cdot IDP\right) \qquad (3)$$

where a and b are empirically determined coefficients, and f_r and f_m are tapers to remove the directivity correction for large distances and low magnitudes. Term f_D is additive (in ln units) to the GMPE median. Distance taper, f_r, is unity for rupture distances $R_{rup} < 40$ km and tapers linearly to zero for $R_{rup} > 70$ km. Magnitude taper, f_m, is unity for $M > 6.0$ and tapers to zero for $M < 5.6$.

Residual Analysis to Investigate Basin and Directivity Effects

We consider here residuals of the modified GMPEs in natural log units, denoted $\varepsilon'(T)$. Those residuals are used directly for the analysis of directivity effects. Residuals from the modified GMPEs are used so that the distance attenuation bias is not mapped into the evaluation of basin and directivity effects. For the analysis of basin effects, we remove the basin correction term from the modified CB GMPE, in which case the residual is denoted $\varepsilon'_{z=0}(T)$. This is done so that trends in residuals can be compared directly to the basin term in the GMPE.

Beginning with directivity, we plot in Figure 4 the variation of residuals with *IDP* for rock sites with R_{rup} < 40 km. Rock sites are used to avoid combining basin effects with directivity, and close distances are used so that we operate below the SC distance taper. Running means and standard deviations are indicated for data grouped into *IDP* bins. The flat trend for PGA indicates a lack of directivity; as period increases the slope of the residuals with *IDP* increases. The SC model provides a good match to the slope of the running means indicated in the figure, especially for the Puente Hill scenario. For the north hypocenter ShakeOut scenario the residuals are relatively lower than other events for *IDP* < 3.0. We believe this results from the slip distribution, which is low at the north end of the fault, where the rupture initiates and *IDP* values are < 3.0.

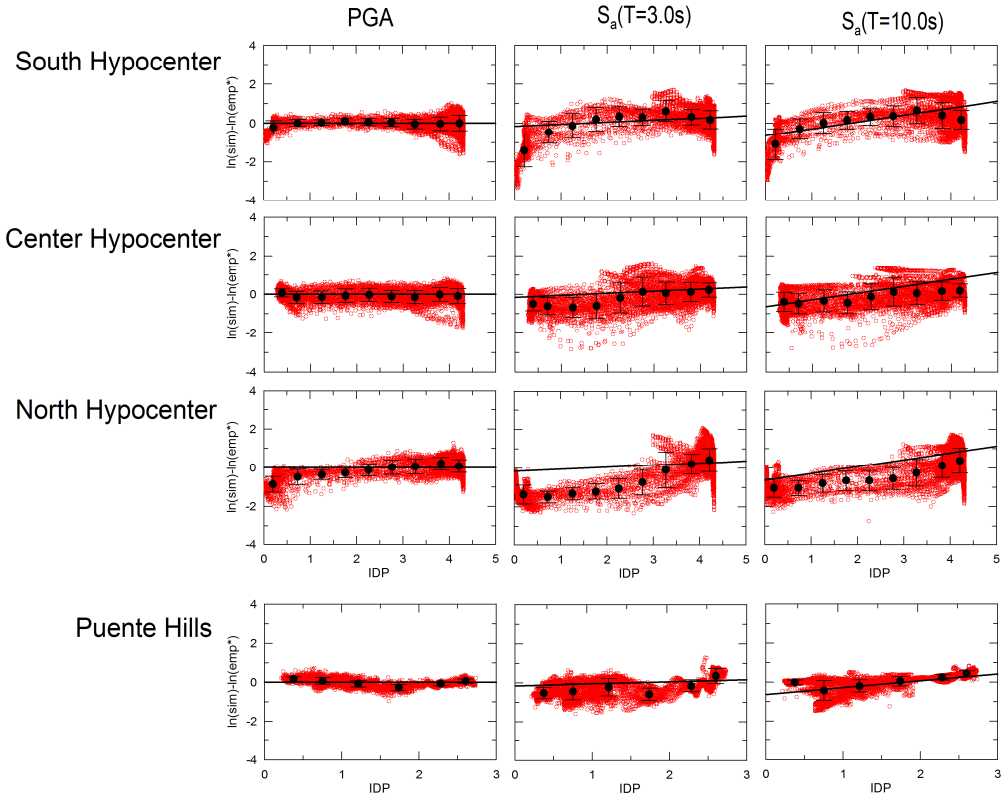

Figure 4. Modified CB residuals for the the ShakeOut scenario as function of IDP for rock sites with R_{rup}<40km. Running means can be compared to trends of SC model.

Figures 5-6 show the modified residuals for rock sites for ShakeOut south hypocenter, and north hypocenter, against rupture distance. The sites are divided into bins of IDP. The trends with distance match the slope of the SC predicted tapers well in some cases, such as South hypocenter bins of IDP < 1 and 2 < IDP < 3 as well as North hypocenter bins of IDP < 1. In other cases the trends with distance are not well matched by the tapers, such as South hypocenter bins of IDP > 3.5, which has trends opposite to the SC taper. Generally for IDP<1 the SC directivity term appears to underpredict the decrease in the mean value of the residuals.

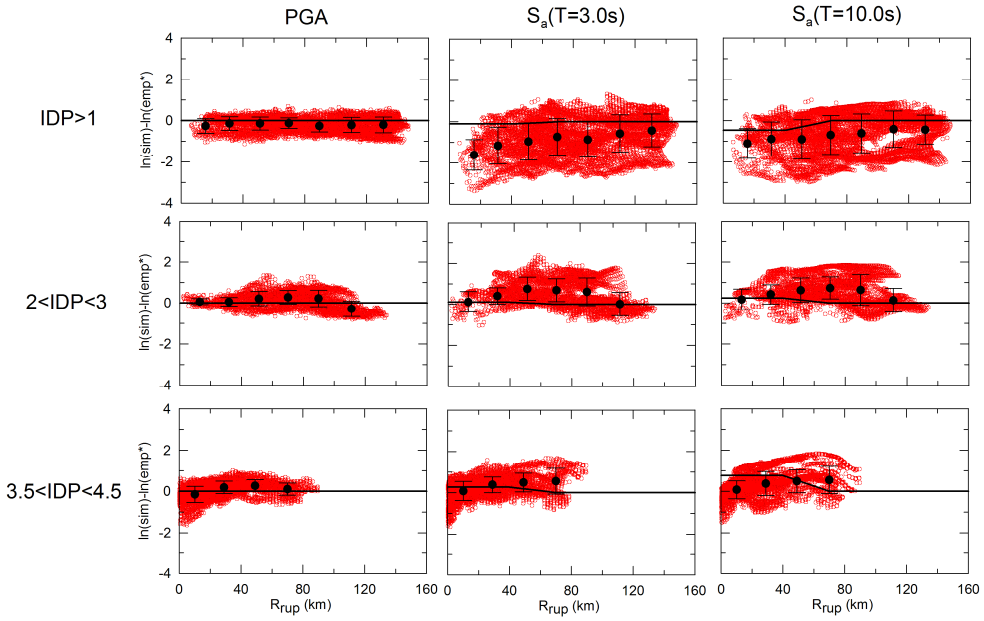

Figure 5. Residuals for ShakeOut motions (original south hypocenter) with modified CB GMPE versus R_{rup} for PGA, SA T=3.0s, and T=10.0s. Results are shown for rock sites for bins of IDP so that trends can be compared to SC predicted distance tapers.

The features observed in Figures 5-6 are not solely related to directivity. The overall size of the residuals and the trends with distance are also affected by the amount of slip on the fault near the sites. For the North hypocenter ShakeOut scenario for the bins of IDP > 3.5 and 2 < IDP < 3 the residuals increase strongly with distance. This is the opposite of the trend predicted by SC. This trend is likely explained by the fact that sites at these IDP levels at long distances from the fault are mostly located near the south end of the fault. The slip prescribed at the south end of the fault is larger than the slip at the north end of the fault. The effect of variation of slip on the residuals may be dominating the directivity effect distance taper that we are trying to examine.

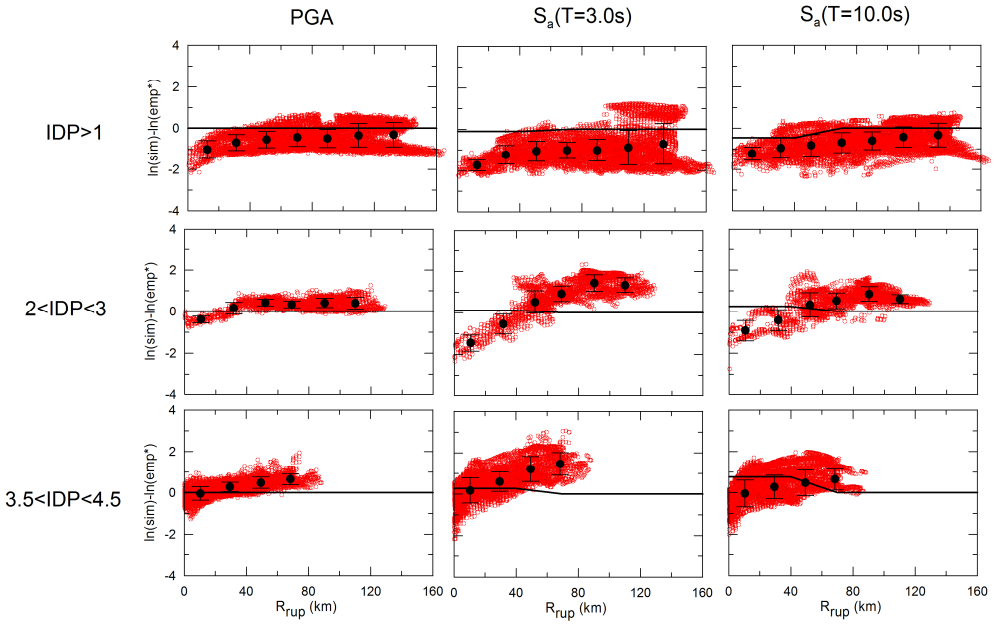

Figure 6. Residuals for ShakeOut motions (North hypocenter) with modified CB GMPE versus R_{rup} for PGA, SA T=3.0s, and T=10.0s. Results are shown for rock sites for bins of IDP so that trends can be compared to SC predicted distance tapers.

Looking next at basin effects, we plot in Figure 7 the variation of residuals with basin depth for T=3.0s S_a for the south hypocenter ShakeOut scenario. Results are shown for six basins: Kern County, San Fernando, Ventura, Los Angeles, San Bernardino, and Imperial Valley. Running means and standard deviations are indicated for data grouped into $Z_{2.5}$ bins. Considering first the south hypocenter ShakeOut event, the CB basin term provides a good match to the slope of the running means for the San Fernando basin, but is too shallow for Los Angeles and appears to have the wrong trend for Imperial. For Los Angeles, the steeper trend indicates that the simulated motions have a faster increase with depth than the empirical model. The reverse trend for Imperial Valley (residuals decrease as $Z_{2.5}$ increases) likely results from the fact that basin depths increase to the south, which also corresponds to decreasing *IDP* and directivity. Hence, the directivity effect may be masking the basin effect in this case.

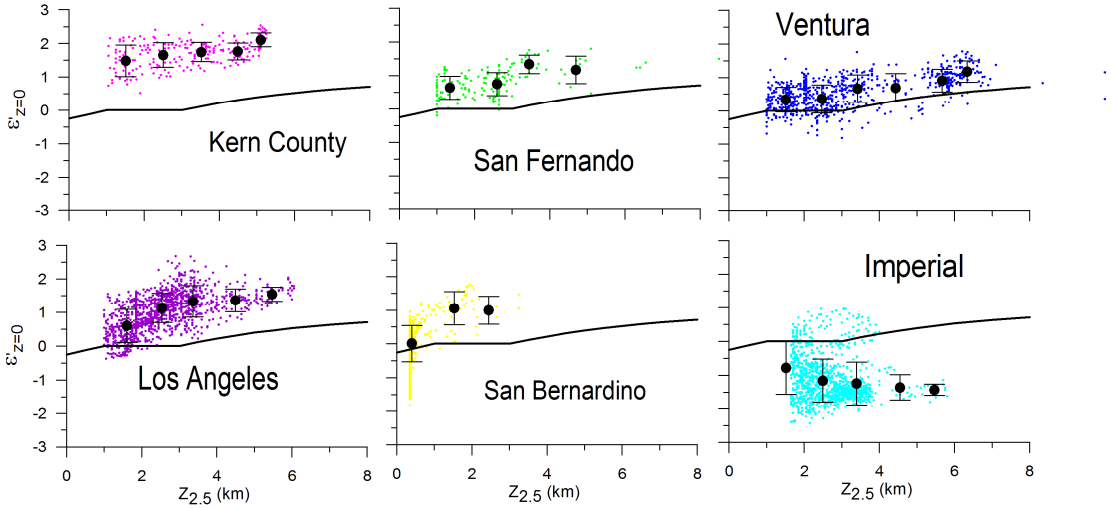

Figure 7. Modified CB residuals for the south hypocenter ShakeOut scenario as function of basin depth. Running means can be compared to trends of basin term in CB GMPE.

Figure 8 shows the modified residuals versus $Z_{2.5}$ for three basins shaken by the Puente Hills earthquake. As with the ShakeOut results, the residuals generally trend upward with respect to $Z_{2.5}$ for each individual basin. For the San Fernando and Ventura basin sites, the simulated model trends are generally similar to those predicted by the GMPE model. The trend for the LA basin sites with $Z_{2.5}$ < 5000 m is stronger than predicted by the GMPE, however for the deeper basin sites the trend drops off and becomes negative. The cause of this trend is not clear.

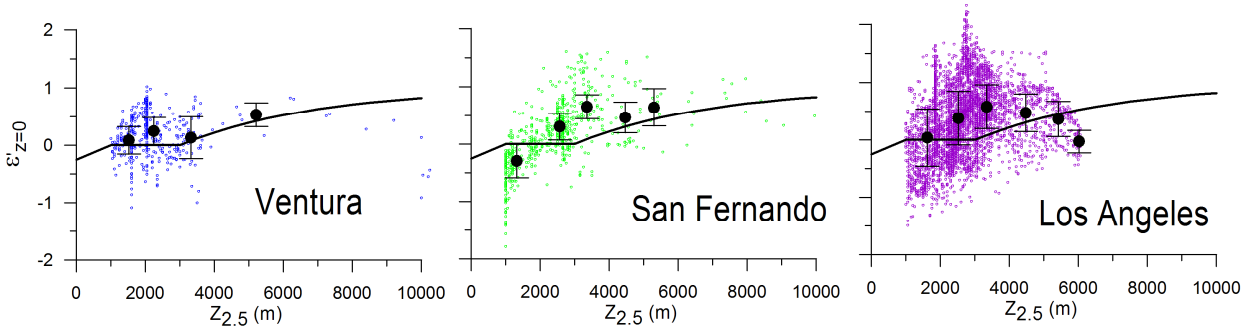

Figure 8. Modified CB residuals for the south hypocenter ShakeOut scenario as function of basin depth. Running means can be compared to trends of basin term in CB GMPE.

Choi et al. (2005) show no significant depth-dependence of residuals for sites in DBL basins (for ShakeOut, these include Los Angeles and San Fernando; for Puente Hills these include San Fernando). That effect is not observed in the present simulations.

Figure 9 shows the ensemble of residuals for each basin along with the mean for the three ShakeOut scenarios. The mean value of the SC directivity term for each basin is also plotted. This figure provides insight into the degree to which directivity effects are coupled with basin effects for these rupture scenarios. For the south and center hypocenter scenario models, the Los Angeles, San Fernando and Ventura basins receive relatively strong ground motions from the channeling of waves from the fault through the basins at low angle (i.e., waves traveling along the fault strike need only turn slightly west to enter the basin). For the North hypocenter scenario, the basin orientation relative to the fault is less favorable, as reflected by a large decrease in the mean value of the residuals for those basins. The Imperial and Kern county basins, at opposite ends of the fault, experience increases and decreases in the mean values of the residuals depending on whether the rupture is towards or away from the basin. The SC directivity term appears to underpredict the increase and decrease in the mean value of the residuals for these two basins. The SC directivity term reflects the general trends described above, but is consistently predicting smaller mean residuals that are produced by the simulations.

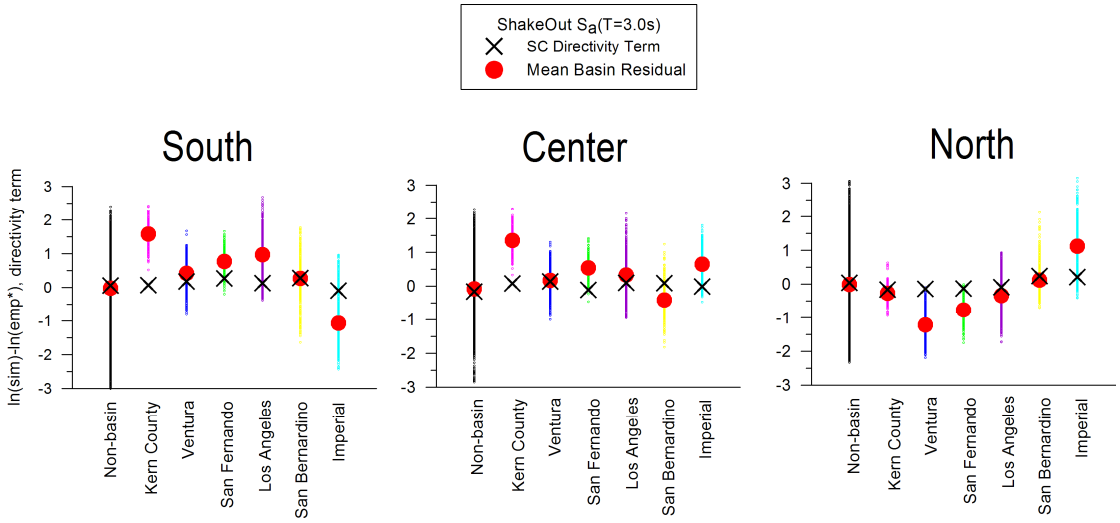

Figure 9: Modified CB residuals for the three ShakeOut scenarios for the major southern California basins. Also shown is the mean value of the SC directivity term.

Conclusions

In this paper we compare the ground motions produced by simulations of major earthquakes on the San Andreas and Puente Hills faults to specific attributes of NGA ground motion prediction equations (GMPEs), in order to investigate basin and directivity effects. We compare the intensity measures (peak acceleration, peak velocity, and spectral acceleration) with those predicted using the NGA GMPEs.

Previous research shows faster distance-attenuation of the simulated data relative to the GMPEs. We modify the GMPE distance attenuation model in order to match the distance the synthetic data so that distance-bias is not mapped into the analysis of other effects.

Analysis of residuals from the modified GMPEs provided insights into basin and directivity effects. We generally observe ground motion increases with depth within basins, but also find complex interactions between basins and fault rupture. Among the most significant of those interactions are relatively strong motions within basins that open to the fault at low angle (i.e., when waves traveling along the fault strike can enter a basin with a small to modest "turn," the basin response is strong). For rock sites, directivity effects at close distance (R_{rup} < 40 km) scale with the isochrone parameter in a manner similar to the Spudich and Chiou (2008) model. The distance tapers included in the SC models do not seem to match well with the synthetic data,

which may be related to more complex factors such as slip distribution on the fault that aren't accounted for in the empirical model. However, the coupling of basin and directivity effects described above often leads to average residuals within basins that are more strongly positive or negative than would be predicted by existing empirical models. It is not clear whether these differences reflect shortcomings in the empirical models or peculiarities in the simulated motions.

References

Abrahamson, N.A. and Silva, W.J., 2008. Summary of the Abrahamson and Silva NGA ground motion relations, *Earthquake Spectra* **24**. 67-97.

Baker J.W., 2007. Quantitative Classification of Near-Fault Ground Motions Using Wavelet Analysis, *Bulletin of the Seismological Society of America*, **97**. 1486–1501.

Boore, D.M. and Atkinson, G.M., 2008. Ground motion prediction equations for the average horizontal component of PGA, PGV, and 5%-damped PSA at spectral periods between 0.01 and 10.0 s, *Earthquake Spectra* **24**. 99-138.

Campbell, K.W. and Bozorgnia, Y., 2008. NGA ground motion model for the geometric mean horizontal component of PGA, PGV, PGD, and 5%-damped linear elastic response spectra for periods ranging from 0.01 to 10 s, *Earthquake Spectra* **24**. 45-55.

Chiou, B.S.-J. and Youngs, R.R., 2008. Chiou and Youngs PEER-NGA empirical ground motion model for the average horizontal component of peak acceleration and pseudo-spectral acceleration for spectral periods of 0.01 to 10 seconds, *Earthquake Spectra* **24**. 173-215.

Choi, Y., Stewart, J.P., and Graves, R.W., 2005. Empirical model for basin effects that accounts for basin depth and source location, *Bulletin of the Seismological Society of America* **95**. 1412-1427.

Graves, R. W., Aagaard, B. T., Hudnut, K. W., Star, L. M., Stewart, J. P., and Jordan, T. H. 2008. Broadband simulations for M_w 7.8 southern San Andreas earthquakes: Ground motion sensitivity to rupture speed, *Geophysical Research Letters* **35**. L22302, doi:10.1029/2008GL035750.

Graves, R., and Pitarka, A., 2004. Broadband Time History Simulation Using a Hybrid Approach. *Proceedings of the 13th World Conference on Earthquake Engineering,* paper no. 1098, Vancouver, Canada.

Graves R. and Somerville, P., 2006. Braodband Ground Motion Simulations for Scenario Ruptures of the Puente Hills Fault, *Proceedings of the 8th U.S. National Conference on Earthquake Engineering,* paper no. 1052, San Francisco, California, USA.

Magistrale, H., Day, S., Clayton, R. W., and Graves R., 2000. The SCEC southern California reference three-dimensional seismic velocity model version 2, *Bulletin of the Seismological Society of America* **90.** 65–76.

Porter et al. 2010. Overview of the ShakeOut Scenario, *Earthquake Spectra*, In preparation.

Power, M., Chiou, B., Abrahamson, N., Bozorgnia, Y., Shantz, T., and Roblee, C., 2008. An overview of the NGA project, *Earthquake Spectra* **24**. 3-21.

Somerville, P.G., Smith, N.F., Graves, R.W., and Abrahamson, N.A., 1997. Modification of empirical strong ground motion attenuation relations to include the amplitude and duration effects of rupture directivity, *Seismological Research Letters* **68**. 199-222.

Spudich, P., and Chiou, B., 2008. Directivity in NGA Earthquake Ground Motions: Analysis using Isochrone Theory, *Earthquake Spectra* **24**. 279–298.

Star, L. M., Stewart, J. P., and Graves, R. W., 2010. Comparison of Ground Motions from Hybrid Simulations to NGA Prediction Equations, *Earthquake Spectra*, In preparation.

Watson-Lamprey, J., and Boore, D., 2007. Beyond Sa_{gmroti} ; conversion to Sa_{arb} , Sa_{sn} , and Sa_{maxrot}, *Bulletin of the Seismological Society of America* **97**. 1511-1524.

Wills, C., Petersen, M., Bryant, W., Reichle, M., Saucedo, G., Tan, S., Taylor G., and Treiman J., 2000. A site conditions map for California based on geology and shear wave velocity, *Bulletin of the Seismological Society of America* **90**. S187-S208.